In situ high-temperature ESR characterization of FeZSM-5 and FeSAPO-34 catalysts in flowing mixtures of NO, C_3H_6, and O_2

A.V. Kucherov *, C.N. Montreuil, T.N. Kucherova * and M. Shelef

Research Laboratory, Ford Motor Company, PO Box 2053, Dearborn, MI 48121, USA
E-mail: mshelef@ford.com

Received 30 September 1998; accepted 16 November 1998

In situ ESR of FeHZSM-5 shows that samples made by sublimation of $FeCl_3$ contain mainly ferric ions in tetrahedral and distorted tetrahedral sites. Above 200 °C these ions do not chemisorb water, which confirms the resistance to activity deterioration by water vapor claimed for FeHZSM-5, when used in SCR of NO_x. The number of ESR-active Fe^{3+} ions decreases when moving from strongly oxidizing conditions towards stoichiometry at 500 °C. In more reducing atmospheres, i.e., when excess reductant is present, the exposure produces an agglomerated ferromagnetic species, presumably magnetite. This process is irreversible. As the trivalent dispersed iron ions are the catalytically active sites, this transformation makes Fe-containing catalysts vulnerable to accidental but irreversible transformation induced by even mildly reducing conditions. The dispersion of ferric ions in FeSAPO-34 is not as good as in FeHZSM-5 and the reactive Fe^{3+} in distorted tetrahedral sites is absent. Catalytic oxidation of ethane allows correlation of the EPR results with activity and stability.

Keywords: ESR, ferric ions, FeZSM-5, ethane oxidation, stability of isolated ferric ions

1. Introduction

Alumosilicates containing non-framework iron have been found to have high activity, poison resistance and durability for selective catalytic reduction (SCR) of nitrogen oxides. Already in 1992, Sato et al. [1] have identified Fe-exchanged zeolites, FeZSM-5 among them, as "the most active" catalysts for selective NO reduction. This was confirmed by Segawa et al. [2] who found FeZSM-5 to be the most active in SCR of NO among a series of cation-exchanged catalysts and resistant to poisoning by water. More recently, Feng and Hall [3,4] announced active and durable FeZSM-5 NO_x SCR catalysts made by ion exchange from oxalate solutions. The results of these experiments were difficult to reproduce in the authors' laboratory as well as in ours. Soon thereafter Chen and Sachtler [5,6] reexamined the FeZSM-5 catalyst in the same reaction using a different preparation procedure, anaerobic sublimation of volatile $FeCl_3$, again noting remarkable poisoning resistance and stability. Then, Kogel et al. [7] used yet another preparation method, solid-state exchange by $FeCl_3$. These publications were generally not in agreement concerning the effects of preparation and pretreatment or even of the origin of the starting FeZSM-5 on activity and stability. Feng and Hall [8] elaborated further on the spatial probability of the presence of bridged iron moieties in ZSM-5, as a function of loading and Si/Al ratio, which are the active sites in their view. Then, Hall and coworkers [9] addressed directly the issue of the FeZSM-5 preparation in a paper entitled "Problems in preparation of FeZSM-5 catalysts". They tried to distinguish between "good" and "poor" catalysts using Mössbauer spectroscopy as the characterization tool. Their message was that, although progress has been made in clarifying some of the puzzling results concerning reproducibility and variability from one laboratory to another, the "problems" of their title have not yet been resolved. They issued a research challenge to other investigators. The present work is relevant to this challenge. In another context, it has been asserted [10] that SAPO-34 is a very thermally stable support for NO_x SCR. For this reason we have included the examination of Fe supported on this zeolite in this study as well.

2. Outline of the work

In response to the above challenge and to gain additional insight into the intriguing behavior of Fe-based SCR catalysts, we have examined the ESR spectra of ferric ions, introduced by sublimation in ZSM-5 and SAPO-34 matrices, in the 20–500 °C temperature range. We have used this experimental technique previously looking at the *in situ* behavior at high temperature of such ions as Cu^{2+} [11,12], Cr^{5+} [13], Rh^{2+} [14] and Gd^{3+} [15]. We have tried to remove as much ambiguity from the results as possible. For this reason, we have (a) adopted Chen and Sachtler's FeZSM-5 preparation procedure [5] as it was shown by these authors that this alleviates all the issues associated with the provenance of the starting zeolite; (b) used the same zeolites employed by us repeatedly in a series of previous publications [11–15]; (c) chosen a Si/Al ratio in the range employed in the work cited above by Feng and Hall/Chen and Sachtler; (d) chosen a high Fe loading

* Permanent address: Zelinsky Institute of Organic Chemistry, RAS, Moscow, Russia.

(Fe/A $\approx$ 0.7) so that it is close enough to previous work yet safely below the appearance of agglomerated iron entities in freshly prepared specimens. Since about $1/3$ of the original protons remain in the sample it is probably better designated as FeHZSM-5. Since we did not expose the samples to durability tests, where residual protons are deemed harmful, these residual protons should not affect our results; (e) used the simple hydrocarbon oxidation reaction to follow the stability of the catalytic activity with treatment; (f) examined the ESR spectra under conditions of NO_x SCR.

3. Experimental

3.1. Sample preparation

Samples of both catalysts were prepared: (a) by sublimating $FeCl_3$ under anaerobic conditions into H-ZSM-5 having a Si/Al ratio of 15 ($SiO_2/Al_2O_3 = 30$), obtained from P & Q Corp., following the procedure described in [5], and (b) by synthesizing SAPO-34 following the procedure enumerated in [16] and similarly sublimating $FeCl_3$ into it. The final Fe loading of both catalysts was $\sim$4 wt% as determined by ICP analysis which is equivalent to an Fe/Al atomic ratio of around 0.7. The samples were pressed without binder, crushed into 0.1–0.2 mm particles and placed in a quartz cell for ESR measurements. Dried samples were precalcined at 500–800 °C in an He + 10% O_2 stream for 2–5 h.

3.2. ESR measurements

The ESR spectra were taken in the X-band ($\lambda \approx 3.2$ cm) at 20–500 °C on a Bruker ESP300 spectrometer, equipped with a high-temperature cavity HT 4114 and a co-axial quartz gas-flow cell [11]. The ESR signals were registered at microwave power 6.4 mW and modulation amplitude 3.8 G in the field range of 50–4,950 G (two scans with a sweep time of 168 s) or 400–2,200 G (four scans with a sweep time of 84 s). The gas flow was regulated by a four-channel readout mass-flow controller (MKS Instruments, model 247C). This system permitted one to vary the composition of the gas mixture by regulating the flow through any of channels from 1.5 to 18 cm^3/min. Pure He (5.0 grade) and the mixtures 10.2 vol% O_2 + He, 0.41 vol% NO + He, 1.0 vol% H_2 + He, and 0.39 vol% C_3H_6 + He were used for *in situ* sample treatment. In some experiments the flow of 10.2 vol% O_2 + He was bubbled through distilled water at 20 °C and this wet gas mixture was used for *in situ* sample treatment at 20–500 °C.

The Bruker ESP300E software and the special Bruker program WIN-EPR (version 901201) were used for data treatment. The Origin 3.5 program for Windows was used for the treatment (baseline correction, noise reduction, double integration) of the recorded spectra.

3.3. Catalytic testing

The catalysts were tested for ethane oxidation [17,18] by placing 95 mg of the sample having 0.25–0.5 mm particles in a fixed-bed quartz microreactor of 0.15 cm^3 volume and treated at 500 °C by dry air flow (50 ml/min) for 2 h. Then the temperature of catalytic run was fixed at a preselected value (>380 °C) and the reactants were fed to the reactor under 1.0 atm pressure. The catalytic activity was measured at ethane conversions from 5 to 70% for a mixture of reactants (90.6 vol% He + 8.4 vol% O_2 + 0.96 vol% C_2H_6) which corresponds to nearly 2.5-fold excess of oxygen. The space velocity was $\sim$22,000 h^{-1}. Samples of the reactor effluent were periodically injected into a chromatograph. Carbon dioxide and water were the major products in all catalytic runs. Traces of ethene were also detected in some runs, for the less active catalysts. A measurable amount of CO (up to 15%) was formed on the FeSAPO-34 sample. This was deduced from the difference in ethane conversion and CO_2 formation. After the initial catalytic runs the catalyst charge was calcined *in situ* in an air stream at 550, 650 and 750 °C for 1 h, and at 800 °C for 2 h. Following these treatments the catalytic tests in the 400–600 °C temperature range were repeated.

4. Results

After calcination FeHZSM-5 shows ESR signals (figure 1(a)) in two different regions of the magnetic field: a weak broad line at $g \approx 2.0$ originating from aggregated, mutually interacting Fe^{3+} ions and intense narrow lines in a low-field region from Fe^{3+} ions in tetrahedral ($g = 4.27$) and distorted tetrahedral ($g = 5.6$ and 6.5) coordinations [19]. This spectrum indicates that the sample preparation resulted in very little agglomerated iron species and we assume that the low-field peaks represent the majority of the iron, although we have not quantified that. This signal is not altered at 500 °C, under oxidizing conditions, save for an intensity decrease due to the Curie–Weiss law. As it was shown earlier, the low-field signal at $g = 5.6$ and 6.5 can be associated with very reactive isolated Fe^{3+}

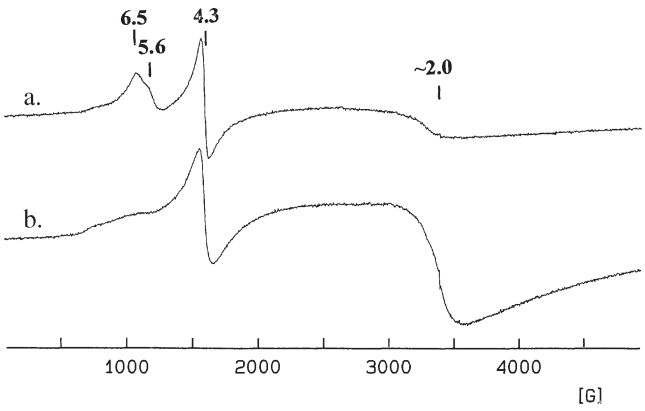

Figure 1. ESR spectra, taken at 20 °C, of (a) FeHZSM-5 and (b) FeSAPO-34 calcined at 500 °C.

cations in distorted tetrahedral coordination [19,20]. This type of cations is easily reducible, and even a weak interaction with inert xenon molecules, filling zeolitic channels at low temperature, is able to displace slightly this type of low-coordinated Fe^{3+} ion in its chelating position [21,22]. It is known that the interaction between H-ZSM-5 and $FeCl_3$ gives rise to stabilization of isolated $(FeCl_2)^+$ species. Subsequent oxidative calcination at 500–550 °C lowers the symmetry of the local crystal field of the ferric cations due to the formation of $(FeO)^+$ species [19]. The ion distribution in FeHZSM-5 is stable after the high-temperature oxidizing treatment: calcination in dry air at 650 and 750 °C for 1 h does not alter noticeably the ESR signal shown in figure 1(a).

If one would adopt the formalistic charge equivalency of one ferric ion to three protons one would expect a considerable excess of extra-lattice iron, which would contribute to iron oxide aggregates. Since the presence of agglomerated species is negligible one can assume that the prevailing Fe/Al atomic ratio, at full exchange, must be unity and the stabilized iron species is $(FeO)^+$.

FeSAPO-34 also shows ESR signals in different regions of the magnetic field (figure 1(b)), but it exhibits a quite intense broad line at $g \approx 2.0$, again originating from mutually interacting Fe^{3+} ions, and a narrower line at $g = 4.27$ identified with tetrahedral coordination. There is a complete absence of the signal from the most reactive low-coordinated Fe^{3+} ions. High-temperature calcination of FeSAPO-34 (750 °C, 1 h) results in some narrowing of the broad line at $g \approx 2.0$ and appearance of a weak shoulder at $g \approx 6.5$. Therefore, no additional aggregation of Fe^{3+} takes place in FeSAPO-34 during calcination; quite the opposite is noted as the dispersion of octahedral interacting Fe^{3+} ions takes place and a small part of low-coordinated Fe^{3+} ions is formed.

Therefore, the two investigated systems, supported on microporous matrices with similar pore geometry but containing disperse iron species of different nature, offer an opportunity for a comparative study of intrinsic activity of Fe^{3+} ions in redox chemistry.

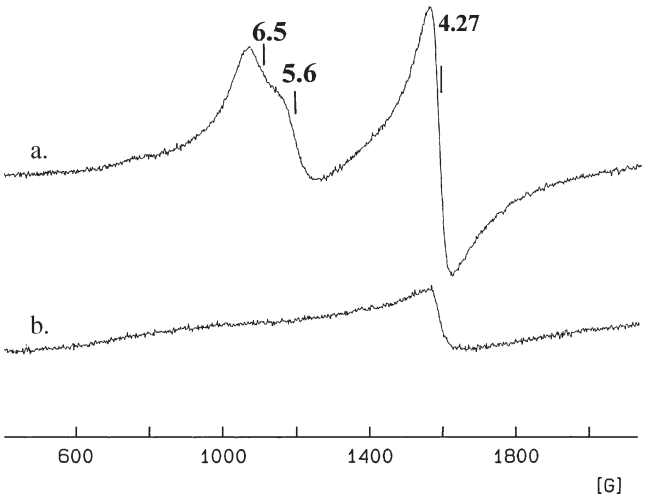

Figure 2. Low-field part of the ESR spectra of FeHZSM-5 taken at 20 °C: (a) dried at 500 °C in He + 10% O_2 flow; (b) after saturation with water vapor from wet He + 10% O_2 flow.

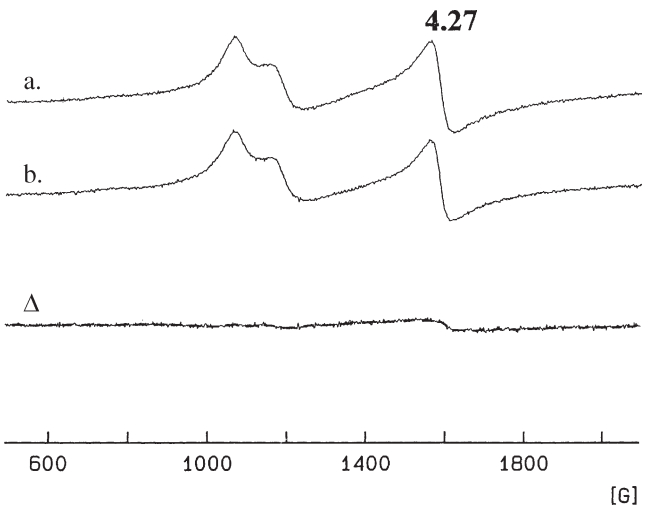

Figure 3. Low-field part of ESR spectra of FeHZSM-5 taken at 200 °C: (a) dried at 500 °C in He + 10% O_2 flow; (b) 20 min after switch to flow of wet He + 10% O_2; (Δ) subtraction of the spectrum (b) from the spectrum (a).

4.1. Interaction of FeHZSM-5 and FeSAPO-34 with H_2O

When FeHZSM-5 is treated at ambient with a flow of wet 10 vol% O_2 + He, the ESR signal associated with the most coordinatively unsaturated ferric ions ($g = 5.6$ and 6.5) disappears and the one at $g = 4.27$ broadens and weakens (figure 2(b)). At the same time, the ESR line at $g = 4.27$ shows an abnormal, sharp temperature dependence of the intensity with cooling observed in prior work [19]. When compared at 77 K, the integral intensity of the line at $g = 4.27$ for the H_2O-saturated sample exceeds the intensity measured for the dry sample by a factor of ∼2. Therefore, the local crystal field symmetry changes from distorted tetrahedral to tetrahedral due to linking of H_2O and, simultaneously, the relaxation conditions for paramagnetic Fe^{3+} sites are affected by water bonding. No narrow line at $g \approx 2.0$, being typical of Fe^{3+} complexes with octahedral symmetry, appears upon saturation of the sample with water. Therefore, the bonding of H_2O ligands with the formation of coordinatively unsaturated structures, even at room temperature, cannot be very strong. This is in contradistinction to the behavior of CuZSM-5 where, at ambient, the ESR signal increases under wet conditions changing the coordination from square-planar to octahedral [22] and the cupric ions are displaced from their cationic positions [23,24].

In the temperature range from 200 to 500 °C no change of the ESR signal from FeHZSM-5 is observed when switching between dry and wet gas flow, indicating a *complete absence* of H_2O chemisorption in this range. Figure 3 illustrates the close coincidence of the two ESR signals at temperature as low as 200 °C. For clarity, the signal differ-

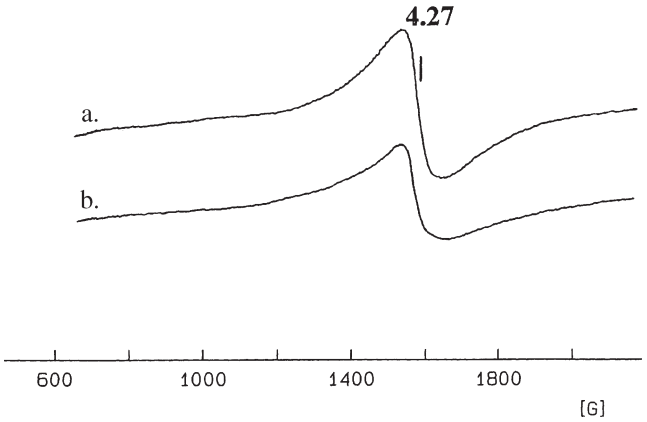

Figure 4. Low-field part of ESR spectra of FeSAPO-34 taken at 20 °C: (a) dried at 500 °C in He + 10% O_2 flow; (b) after saturation with water vapor from wet He + 10% O_2 flow.

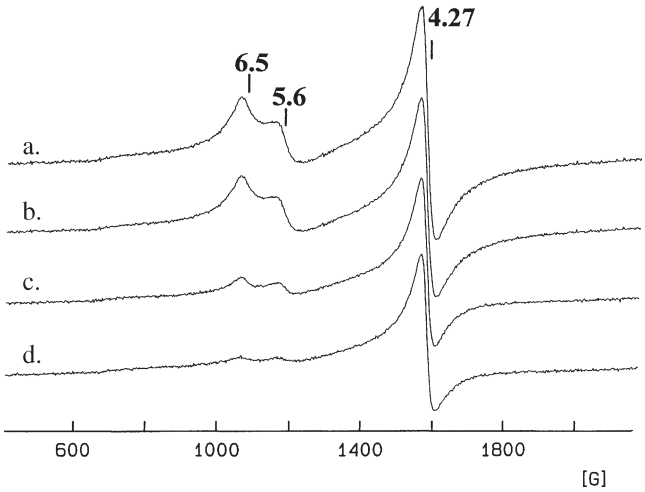

Figure 5. Change in low-field part of the ESR spectra of FeHZSM-5 caused by stepwise sorption of NO at 20 °C: (a) starting signal, pure He flow; (b) ∼1 min after switch to He + 0.4% NO flow; (c) 5 min in flow; (d) 15 min in flow.

ence (Δ) is shown in figure 3, being the result of subtraction of the two ESR spectra taken at 200 °C in dry and wet gas flow (figure 3 (a) and (b)). Again, this is in contradistinction to the behavior of CuZSM-5, where some influence of water vapor on the shape of the Cu^{2+}-ESR signal is seen even at 400 °C, pointing to a much stronger interaction of the active sites with H_2O molecules. This result is of direct relevance to the claimed resistance [2,4,5] to the suppression of NO_x SCR activity of FeZSM-5 as opposed to that of CuZSM-5, the latter being much more susceptible to instantaneous water inhibition. We would like to point out that the ferric ion in the cationic position is not "hydrophobic", as designated by some workers [9]. More accurately, it coordinates water weakly at ambient conditions and not at all at the SCR conditions. The interaction of iron ions in FeSAPO-34 with water vapor is quite weak at 20 and 100 °C, and becomes negligible at $T > 200$ °C. Only the ESR signal from isolated tetrahedral Fe^{3+} ions, with $g = 4.27$ is affected somewhat by H_2O sorption, as shown in figure 4. As one can expect, no measurable change of the broad ESR line at $g \approx 2.0$ from interacting (clustered) Fe^{3+} ions is induced by water even at ambient conditions.

4.2. Interaction of NO and NO_2 with FeHZSM-5 and FeSAPO-34

At ambient, under dry conditions, NO gradually suppresses the signal from the most coordinatively unsaturated ferric ions in FeHZSM-5 (figure 5), presumably due to pairing of spins between the unpaired electron on the NO and that on Fe^{3+}. An increase in the Fe^{3+} site symmetry accompanies this bonding. Subsequent sample purging at 20 °C by pure He flow does not restore the ESR signal (figure 5(d)). This provides evidence of quite strong linking between the coordinatively unsaturated Fe^{3+} active site and the NO molecule. Treatment of the FeHZSM-5 at ambient with NO + O_2 flow, i.e., NO_2 sorption, also results in an irreversible disappearance of the ESR lines at $g = 5.6$ and 6.5 due to formation of complexes with higher symmetry. However, at temperatures typical of the SCR reaction conditions (400–500 °C), NO has a negligible effect on the ESR signal from FeHZSM-5. No interaction with NO or NO + O_2 affecting the Fe^{3+}-ESR signal from FeSAPO is detected even at 20 °C. Thus, Fe^{3+} sites stabilized by this matrix have a lesser affinity towards NO and NO_2 ligands.

4.3. Reduction of FeHZSM-5 and FeSAPO-34 with C_3H_6 and H_2

At room temperature, in an He + propene flow a gradual disappearance of the low-field Fe^{3+}-ESR lines ($g = 5.6$ and 6.5) points to interaction of coordinatively unsaturated sites in FeHZSM-5 with olefin molecules. It is an open question, whether formation of a more symmetric complex takes place or the reduction of Fe^{3+} to Fe^{2+} proceeds at room temperature. Heating of the sample with the olefin sorbed at 250 °C for 10 min results in complete disappearance of the lines from Fe^{3+} ions but reoxidation of the sample at 500 °C restores the starting ESR spectrum of figure 1(a). If the sample, with olefin sorbed, is heated at 400 °C a new, very broad ESR line ($\Delta H > 2{,}500$ G, $g \approx 2.2$) appears, pointing unambiguously to the formation of a ferromagnetic phase. Even prolonged reoxidation of such a sample at 500–550 °C does not result in restoration of the parent ESR signal from the Fe^{3+} ions. The same effect is seen after treatment of the FeHZSM-5 with an He + H_2 stream. At 300 °C, a switch to an He + 1% H_2 flow for 5 min causes a relatively small change in the ESR signal originating from Fe^{3+} ions, and restoration of the parent ESR spectrum occurs after a back switch to He + 10% O_2. At 400 °C the same treatment results in an irreversible loss of the ESR signal from the Fe^{3+} ions, accompanied by the appearance and gradual increase of a very broad line of ferromagnetic resonance (figure 6(a)). However, appearance of this line is not to be taken as due to the formation of Fe^0 particles. A magnetite phase, Fe_3O_4, can also be responsible for the observed ferromagnetism. A more detailed, quanti-

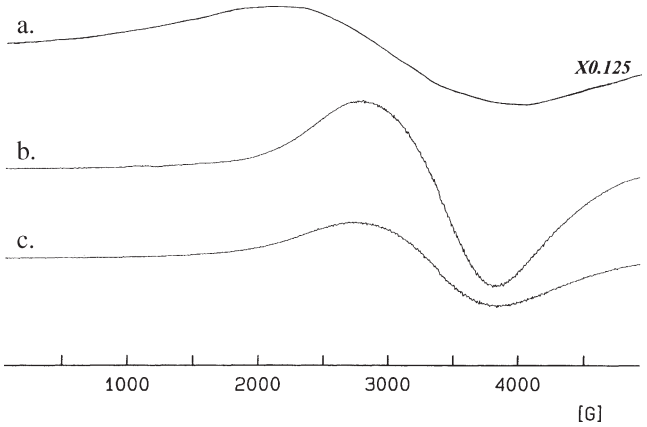

Figure 6. ESR spectra, taken at 400 °C, for FeHZSM-5: (a) after 30 min in He + 1% H_2 flow; (b) after reoxidation by He + 10% O_2 flow for 500 °C for 1.5 h; (c) after 2 h in $O_2 + CCl_4$ flow.

tative measurement of magnetic susceptibility could clarify this point, but for now formation of Fe_3O_4 seems to be a more plausible explanation, as it is repeatedly noted that iron in FeHZSM-5 cannot be reduced to Fe^0 up to 800 °C [4,6]. In any case, ferromagnetism being a collective property, it gives unambiguous evidence of *agglomeration of iron ions* in our sample as a result of reductive treatments at temperatures $\geqslant$400 °C, i.e., relatively mild conditions.

A prolonged reoxidation, at 500 °C, of the sample prereduced by H_2 does not lead to restoration of the parent ESR signal with low-field lines from Fe^{3+} ions (figure 1(a)), but results in the formation of the spectrum shown in figure 6(b). This newly formed, symmetric ESR line, with $g \approx 2.0$ and $\Delta H \approx 1{,}000$ G, is indicative of the transformation of ferromagnetic Fe_3O_4 to α-Fe_2O_3 particles by oxidation. It is important to note that even oxidation at 600 °C for 3 h does not lead to the appearance of the ESR signal from low-coordinated Fe^{3+} ions. Therefore, even severe high-temperature treatment does not disaggregate the aggregated particles. There is no migration of cationic Fe^{3+} species back to starting positions. This is in agreement with an earlier observation that a temperature of 550–600 °C is too low to induce solid-state migration of Fe^{3+} ions from bulk particles of iron oxides to cationic positions inside zeolitic channels [19].

Hence, the ESR-observable Fe^{3+} sites can be reversibly oxidized after a mild reduction to Fe^{2+} ions but a more severe reduction, with the formation of aggregated ferromagnetic particles (probably on the outer surface of the zeolite crystals), causes irreversible redistribution of iron.

Thermal treatment of the sample with an $O_2 + CCl_4$ flow was tried in an attempt to restore the ESR spectrum of the FeHZSM-5 altered by the reductive treatment. It was shown earlier that the presence of CCl_4 molecules enhances the "solid-state" introduction of polyvalent ions into zeolites, due to a sharp increase in the mobility of the cationic fragments by *in situ* formation of active species. In some cases, this chemical transport reaction, with the formation of reactive and mobile oxychloride fragments, provides for effective disaggregation of the oxide phase and results in migration of active species into zeolitic channels under mild conditions [25].

Sample treatment *in situ* by an $O_2 + CCl_4$ flow at 200–250 °C resulted in slow, minor changes in the spectrum (figure 6(b)), so the temperature was increased to 400 °C. A gradual decrease in the signal intensity during the treatment demonstrates progressive dispersion of the iron oxide. Nevertheless, the process is not very effective, and after 2 h of treatment, $\sim$40% of the initial amount of the Fe_2O_3 is still present in the sample (figure 6(c)). An increase of the temperature to 500–550 °C results in a rather fast quantitative disappearance of the ESR line originating from the Fe_2O_3 phase. Hence, under such conditions, sublimation of iron undoubtedly takes place and the sample is bleached while a colored ring appears on the quartz wall in a cold part of the ampoule. This iron transfer demonstrates that the CCl_4-assisted high-temperature process is mediated through the gas phase, with the formation of volatile species. However, no restoration of Fe^{3+} ions into the reactive low-coordinated sites of H-ZSM-5 was achieved.

FeSAPO-34 demonstrates the same kind of transformations upon redox treatment: the Fe^{3+} ESR signal is reversible when the sample is reduced at 250–300 °C for a few minutes, but a more severe reduction, leading to formation of ferromagnetic particles, causes irreversible redistribution of iron.

4.4. High-temperature interaction of FeHZSM-5 and FeSAPO-34 with $O_2 + NO + C_3H_6$ gas mixtures

The dynamics of the Fe^{3+} sites in FeHZSM-5 and FeSAPO-34 during the catalytic process of SCR at realistic temperatures is of the most direct relevance to the comparative study of the behavior of catalytic sites. Earlier, this same approach was adopted for the study of Cu^{2+}- and Cr^{5+}-catalytic sites in H-ZSM-5 [12,13]. To this end, we followed the *in situ* C_3H_6 oxidation by O_2 + NO at 500 °C in gas mixtures with varying ratios of gas components. The overall gas flow rate He + O_2 + NO + C_3H_6 was maintained at 15 cm^3/min, the NO concentration was fixed at 0.08 vol%, and the inlet of oxygen and propene ratios were varied in a wide range. When the gas flow is switched from He + O_2 to the complex mixture containing both the oxidants and the reductant, the dynamic steady-state is established in less than 3 min, and the drop in the ESR signal intensity reflects quantitatively the extent of Fe^{3+} reduction.

Figure 7(a) shows the ESR spectrum of FeHZSM-5 taken at 500 °C in a flow of He + 10% O_2. A switch of the gas flow to a strongly oxidizing propene-containing mixture (X = oxidant/propene stoichiometric ratio of $>$10) does not change the signal at all. This is in complete agreement with the Mössbauer results [9] that after exposure to oxidizing conditions of SCR virtually all iron is trivalent.

The most accurate comparison of the ESR spectra by subtraction confirms the lack of measurable Fe^{3+} reduction (accuracy of $\pm$3%). Shifting the gas composition nearer to

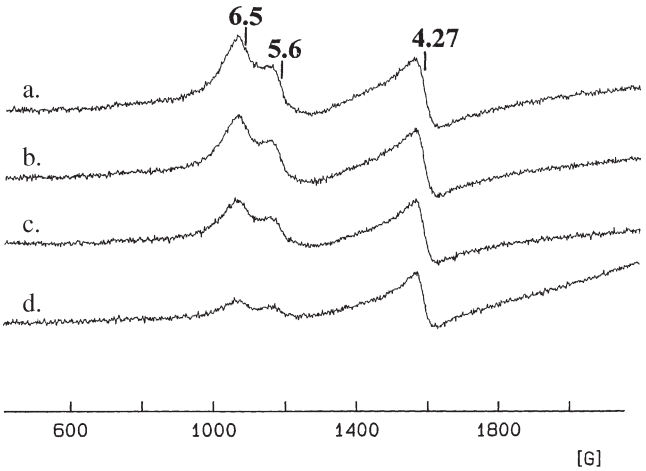

Figure 7. Transformations of the low-field part of the ESR spectra of FeHZSM-5, at 500 °C, caused by change in the composition of the gas mixture $He + O_2 + NO + C_3H_6$: (a) stoichiometric ratio, $X = (O_2 + NO)$/propene, between 110 and 9.2; (b) $X = 1.5$; (c) $X = 1.2$; (d) $X = 0.92$, ∼3 min.

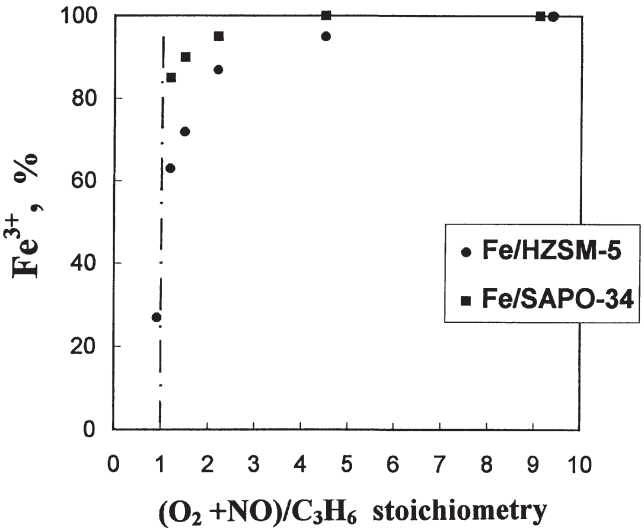

Figure 8. Relative concentration of Fe^{3+} ions in FeHZSM-5 and FeSAPO-34 vs. stoichiometric ratio, X = oxidant/propene, in the gas mixture $He + O_2 + NO + C_3H_6$ at 500 °C.

stoichiometry leads to a gradual decrease in the intensity of the signal from Fe^{3+} ions (figure 7(b), $X = 1.5$, signal loss ∼30%; figure 7(c), $X = 1.2$, signal loss ∼40%). Thus, a measurable reduction of the Fe^{3+} takes place under a low excess of oxygen, and the most coordinatively unsaturated ions are reduced first. This dynamic equilibrium $Fe^{3+} \leftrightarrow Fe^{2+}$ is completely reversible: backswitching the gas flow to $He + O_2$ restores the parent signal fast (figure 7 (c) → (a)). But the decrease in the oxidant/propene ratio below stoichiometry induces a sharp and irreversible change in the catalyst state: a fast disappearance of the Fe^{3+}-ESR signal (figure 7(d)) is accompanied by the formation of a very broad line of ferromagnetic resonance due to an aggregation of iron ions into a magnetite-like phase, and, again, restoration of the parent ESR signal cannot be achieved after reoxidation. This behavior confirms the reduction experiments with the olefinic residue and with hydrogen described above. It underscores the vulnerability of FeHZSM-5 to inadvertent reducing conditions.

At 500 °C in a flow of $He + O_2 + NO + C_3H_6$ at different stoichiometries, going from oxidizing to reducing conditions, the Fe^{3+}-ESR signal from FeSAPO-34 at $g \approx 2.0$ shows a gradual *decrease* when going from a stoichiometric ratio $(O_2 + NO)/C_3H_6$ of 9 down to 1.2. However, this dependence is not as sharp as in the case of FeHZSM-5. Thus, in FeSAPO-34 the octahedral, presumably agglomerated, form of ferric ions is both more prevalent and, although accessible to reduction, it is substantially less reactive.

Figure 8 summarizes the relations between the concentrations of the Fe^{3+} ions and the oxidant/propene ratio for both catalysts. It is clear that the H-ZSM-5 matrix provides stabilization of a part of Fe^{3+} ions in a much more reactive state, as compared with the SAPO-34 matrix but this stabilization is vulnerable to irreversible transformation reducing conditions.

4.5. Catalytic activity of FeHZSM-5 and FeSAPO-34 in ethane oxidation

The catalytic activity of pure H-ZSM-5 or SAPO-34 in ethane oxidation is negligible up to 550 °C. The introduction of iron creates catalytically active sites. The activity of iron-containing samples reaches a steady state within the first 15 min on stream and no change in effectiveness of the catalysts is noted after 3 h of continuous use.

The conversion of ethane to CO_2 on samples calcined at different temperatures is presented in figure 9 (a) for FeHZSM-5 and (b) for FeSAPO-34 as a function of the reaction temperature. The activities of the samples differ sharply and direct comparison of all experimental data at one fixed temperature (500 °C, for example) is not permissible, because the conversion is too high for the more active FeHZSM-5. Therefore, we plotted our data in coordinates of the Arrhenius equation and extrapolated the results for FeSAPO-34 to lower temperatures and conversions, as done in previous work [17,18]. These data are used for comparison of activities at a constant temperature of 440 °C, at conversion values of <15% for all the samples. As the catalysts contain several different types of iron ions, the calculation of a specific reaction rate, per one Fe^{3+} ion, makes no physical sense. Therefore, overall conversions, associated with the total amount of iron, are compared at a fixed temperature, for identical sample charges and same gas flow.

Figure 10 shows the change in activity of the two samples after stepwise calcination. As mentioned, introduction of iron into catalytically inactive supports creates active sites for ethane oxidation and the activities of FeHZSM-5 and FeSAPO-34 differ sharply. This is particularly apparent for the samples calcined at 500–650 °C (figures 9, 10). The pore structure of the two microporous supports is almost identical and, hence, the geometrical/diffusion factor

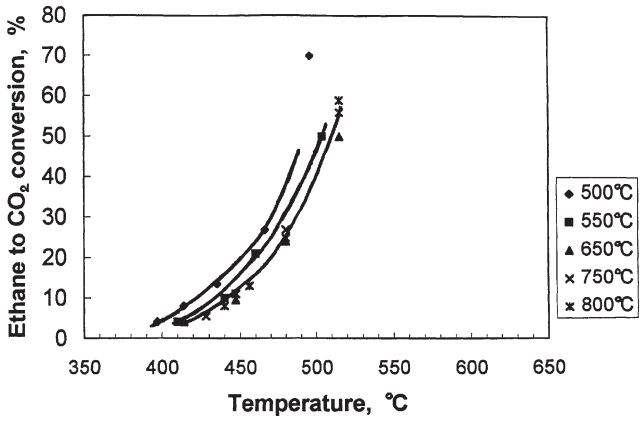

(a)

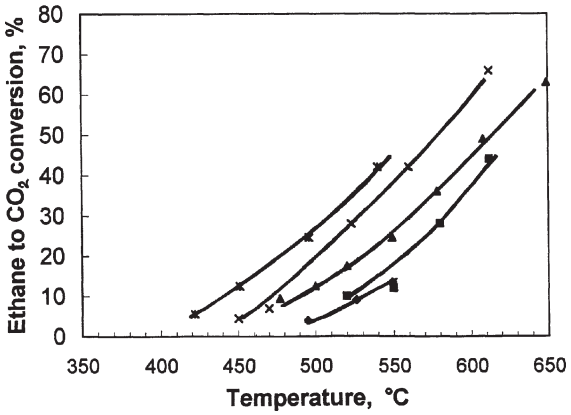

(b)

Figure 9. Ethane to CO_2 conversion vs. reaction temperature for (a) FeHZSM-5 and (b) FeSAPO-34 calcined at 500–800 °C.

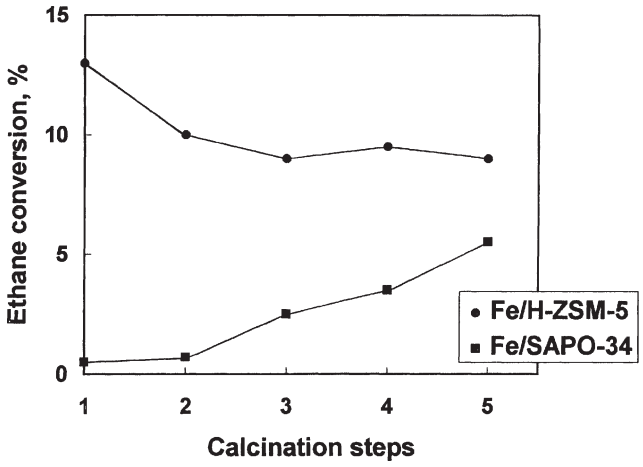

Figure 10. Change in specific catalytic activity of Fe^{3+} sites (ethane oxidation at 440 °C) in FeHZSM-5 and FeSAPO-34 caused by stepwise calcination: 1 – 500 °C, 2 h; 2 – 550 °C, 1 h; 3 – 650 °C, 1 h; 4 – 750 °C, 1 h; 5 – 800 °C, 2 h.

is of little significance in the comparison of catalytic activities which differ by more than an order of magnitude. The difference in the catalytic activity between FeHZSM-5 and FeSAPO-34 is caused mainly by the difference in the intrinsic properties of Fe^{3+} sites stabilized by the two supports. It is plausible that not only the reaction rates but also the reaction mechanisms differ for the two catalysts. This possibility is indicated by two experimental results: (1) on the less active FeSAPO-34, with aggregated iron species, a noticeable amount of CO is formed; (2) comparison of the slopes of the catalytic curves (figure 9) points to a significant difference in apparent activation energies: 32 and 39 kcal/mol for FeHZSM-5 and FeSAPO-34, respectively.

It was shown above that the high-temperature calcination of FeHZSM-5 up to 800 °C does not cause a noticeable change in the mode of iron ion stabilization by H-ZSM-5 matrix (figure 1(a)). This is in good agreement with the high stability of this catalyst, after high-temperature treatments, in ethane oxidation (figure 10). The stepwise increase in activity of FeSAPO-34 upon calcination agrees with the increase in dispersion of iron oxide species and appearance of a certain amount of isolated reactive Fe^{3+} ions observed by ESR. This point requires more quantitative work. As a whole, the results obtained for the catalytic oxidation of ethane agree well with the observed ESR features of Fe^{3+} sites in the two examined supports, indicating a much higher redox activity of a part of iron cations in FeHZSM-5.

4.6. Effect of lanthanide stabilizers on FeHZSM-5

It was shown in previous work that introduction of lanthanides in CuHZSM-5 can improve, to some extent, the catalyst resistance against high-temperature deactivation by dealumination [26,27]. In our recent work we proposed to use the paramagnetic Gd^{3+} ion as a surrogate in ESR studies of lanthanide distribution in multi-component catalysts [14,15]. Here we applied the same approach for FeHZSM-5. Gadolinium (5 wt%) was introduced into the FeHZSM-5 by a two-fold impregnation from nitrate solution with subsequent calcination in air flow at 500 °C for 5 h. Mono-cationic 5 wt% GdHZSM-5 was prepared from H-ZSM-5 for comparison. The mono-cationic sample shows a quite complex ESR spectrum being a superposition of signals from several forms of Gd^{3+}: (1) rigidly bonded isolated Gd^{3+} ions, (2) very small Gd^{3+} clusters (containing only a few ions) capable of interacting with water molecules, (3) excess Gd as non-dispersed, particulate oxide. It was shown earlier that Gd^{3+} ions do not block the cationic positions of H-ZSM-5 from further interaction with paramagnetic Cu^{2+} or Rh^{2+} cations [14] and a similar conclusion is apparent from our study of (GdFe)HZSM-5. The ESR signals from this multi-cationic sample represent a simple superposition of the two individual spectra, from Fe^{3+} and Gd^{3+}, and no change in behavior of Fe^{3+} sites upon interaction with different ligands (H_2O, NO, C_3H_6) is caused by the presence of gadolinium.

5. Discussion

The underlying assumption in this discussion is that the trivalent ferric ions are the active sites in FeHZSM-5 both

in the oxidation of ethane which we have used as a probe reaction in this work as well as in SCR. This is in agreement with Hall et al. who introduced the iron in the divalent state and had determined by Mössbauer spectroscopy that in the working SCR catalyst, at a substantial excess of the oxidants, almost all the iron is present as Fe^{3+} [9]. The sublimation method of catalyst preparation introduces the trivalent ions to begin with and these prevail and are observed by ESR as long as the overall conditions are fairly oxidizing. Reducing conditions at temperatures >400 °C induce an irreversible agglomeration of a magnetic phase, presumably containing both Fe^{2+} and Fe^{3+} ions. The "poor" catalyst of Hall et al. [9] shows some agglomeration when treated in a "neutral" He flow at >400 °C. Would the switch to a reducing atmosphere have done the same to the "good" catalyst? Other instances of agglomeration of iron into a magnetic phase in zeolites are mentioned in the literature. Lazar et al. [28] observed nanometer size magnetite particles in FeY zeolites, while Goldfarb et al. [29] observed agglomeration of Fe^{3+} ions in Fe-faujasites during dehydration/rehydration cycling. This should not, in retrospect, be surprising as the anchoring of trivalent ions into cationic sites is known to be relatively weak. While the materials are very stable under oxidizing conditions and the ferric ions are not dislodged by rare-earth ions, the high-temperature exposure to *mildly* reducing conditions damages the active sites irreversibly. Such conditions are virtually unavoidable in automotive applications but might be of lesser consequence in stationary pollution control. The irreversibility of the agglomeration process is also in agreement with the fact that the introduction of ferric ions into zeolites by solid-state exchange does not proceed by migration of the oxide, but requires the mediation of a volatile halide. We are not certain whether the notorious irreproducibility of the activity tests of FeZSM-5 in NO_x SCR is the outcome of adventitious irreversible agglomeration of the ferric ions, but it does seem as good a reason as any.

The observable ESR signal, associated with the unpaired electrons of the ferric ions, suggests that these latter are not a part of assemblies of multiple ions. Feng and Hall [8] have postulated an oxygen-bridged pair of ferrous cations and have calculated the geometrically allowed probability of their existence is a function of Fe-loading and the Si/Al ratio. Their calculations show that in a FeZSM-5, such as used in this work, the probability of forming $(Fe–O–Fe)^{2+}$ pairs is >0.5. Chen and Sachtler [6] also propose a paired oxygen-bridged active site but in their case it contains a hydroxyl group associated with each ferric ion $[(HO)Fe–O–Fe(OH)]^{2+}$. The reason for proposing a paired dicationic active site is to rationalize a simple path for a concerted transfer of a doubly charged oxygen ion during the reduction step. Hall et al. [9] acknowledge that these suggestions do not adequately define the active site.

Another question that immediately arises is whether the observable ESR signals, which we associate with the active sites, may originate from either of the proposed paired complexes. At present we do not have an answer, but it does appear improbable that a moiety containing two identical cations will be spatially arranged so as to preclude the pairing of the unpaired electrons of the individual ions.

6. Conclusions

(1) *In situ* ESR at operating catalyst temperatures has been applied to yet another ESR active ion (Fe^{3+}) in zeolites providing additional insight into its catalytic properties.

(2) The ferric ions in FeHZSM-5 situated in tetrahedral sites are stable under oxidizing conditions up to quite high temperatures of the order of 800 °C. They are active in the oxidation of ethane under excess oxygen. They coordinate H_2O only weakly and, above 200 °C, their ESR signal is unaffected by the presence of water, in contrast to the effect of water on cupric ions in CuHZSM-5. This supports the repeatedly reported lesser sensitivity of FeHZSM-5 to instantaneous deactivation by water.

(3) At the common temperatures of the catalytic process >400 °C the Fe^{3+} ions are irreversibly agglomerated to a ferromagnetic phase (presumably magnetite) under only slightly reducing conditions. This is observed when the reductants are olefinic residues present on the catalyst, hydrogen in the gas phase or a hydrocarbon in the reacting gas stream. This underscores the vulnerability of these catalysts to an unintended exposure to reducing conditions.

(4) The dispersion of ferric ions in FeSAPO-34 is not as good as in FeHZSM-5 and the reactive Fe^{3+} in distorted tetrahedral sites is absent.

Acknowledgement

We thank Mohinder Chattha and Bob Kudla for the preparation of the samples and discussions of the project.

References

[1] S. Sato, H. Hirabayashi, H. Yahiro, N. Mizuno and M. Iwamoto, Catal. Lett. 12 (1992) 193.
[2] K. Segawa, K. Watanabe and R. Kunugi, Trans. Mater. Res. Soc. Jpn. A 15 (1994) 131.
[3] X. Feng and W.K. Hall, Catal. Lett. 41 (1996) 45.
[4] X. Feng and W.K. Hall, J. Catal. 166 (1997) 368.
[5] H.-Y. Chen and W.M.H. Sachtler, Catal. Lett. 50 (1998) 125.
[6] H.-Y. Chen and W.M.H. Sachtler, Catal. Today 42 (1998) 73.
[7] M. Kogel, V.H. Sandoval, W. Schwieger, A. Tissler and T. Turek, Catal. Lett. 51 (1998) 23.
[8] X. Feng and W.K. Hall, Catal. Lett. 46 (1997) 11.
[9] W.K. Hall, X. Feng, J. Dumesic and R. Watwe, Catal. Lett. 52 (1998) 13.
[10] T. Ishihara, M. Kagawa. F. Hadama and Y. Takita, J. Catal. 169 (1997) 93.
[11] A.V. Kucherov, J.L. Gerlock, H.-W. Jen and M. Shelef, J. Phys. Chem. 98 (1994) 4892.
[12] A.V. Kucherov, J.L. Gerlock, H.-W. Jen and M. Shelef, J. Catal. 152 (1995) 63.
[13] A.V. Kucherov, C.P. Hubbard and M. Shelef, Catal. Lett. 33 (1995) 91.

[14] S.G. Lakeev, A.V. Kucherov and M. Shelef, Appl. Catal. B 16 (1998) 245.
[15] A.V. Kucherov, A.A. Slinkin and M. Shelef, Catal. Lett. 50 (1998) 1.
[16] US Patent No. 4,440,871 (1984).
[17] A.V. Kucherov, C.P. Hubbard, T.N. Kucherova and M. Shelef, Appl. Catal. B 7 (1996) 285.
[18] A.V. Kucherov, T.N. Kucherova and A.A. Slinkin, Catal. Lett. 10 (1991) 289.
[19] A.V. Kucherov and A.A. Slinkin, Zeolites 8 (1988) 110.
[20] A.A. Slinkin and A.V. Kucherov, Catal. Today 36 (1997) 485.
[21] A.V. Kucherov and A.A. Slinkin, J. Phys. Chem. 93 (1989) 864.
[22] A.V. Kucherov, J.L. Gerlock, H.-W. Jen and M. Shelef, Zeolites 15 (1995) 9.
[23] M.W. Anderson and L. Kevan, J. Phys. Chem. 91 (1987) 4174.
[24] C.E. Sass and L. Kevan, J. Phys. Chem. 92 (1988) 5192.
[25] A.V. Kucherov, T.N. Kucherova and A.A. Slinkin, Catal. Lett. 10 (1991) 289.
[26] M.J. Rokosz, A.V. Kucherov, H.-W. Jen and M. Shelef, Catal. Today 35 (1997) 65.
[27] P. Budi, E. Curry-Hyde and R.F. Howe, Catal. Lett. 41 (1996) 47.
[28] K. Lazar, G. Pal-Borbely, H.K. Beyer and H.G. Karge, in: *Preparation of Catalysts VI*, eds. G. Poncelet et al. (Elsevier, Amsterdam, 1995) pp. 551–559.
[29] D. Goldfarb, M. Bernardo, K.G. Strohmaier, D.E.W. Vaughan and H. Thomann, J. Am. Chem. Soc. 116 (1994) 6344.